

<sup>22</sup>A. K. Common and M. K. Pidcock, Nucl. Phys. **B42**, 194 (1972); P. Grassberger, *ibid.* **B42**, 461 (1972); A. K. Common, Nuovo Cimento **56A**, 524 (1968).

<sup>23</sup>A. Martin, Nuovo Cimento **47A**, 265 (1967).

<sup>24</sup>G. F. Chew and S. Mandelstam, Phys. Rev. **119**, 467 (1960); G. F. Chew, S. Mandelstam, and H. P. Noyes, *ibid.* **119**, 478 (1960).

<sup>25</sup>M. R. Pennington and S. D. Protopopescu, Phys. Letters **40B**, 105 (1972); M. R. Pennington and C. Schmid, LBL Report No. LBL-1005, 1972 (unpublished).

<sup>26</sup>D. Morgan and G. Shaw, Phys. Rev. D **2**, 520 (1970); D. Morgan, *Springer Tracts in Modern Physics*, edited by G. Höhler (Springer, New York, 1970), Vol. 55, p. 1.

<sup>27</sup>H. Kühnelt, Z. Physik **246**, 447 (1971); F. Widder, Acta Phys. Austr. **34**, 264 (1971); O. Piguet and G. Wanders, Nucl. Phys. **B46**, 295 (1972).

<sup>28</sup>This is the most appropriate amplitude for these considerations.

<sup>29</sup>The Lovelace-Veneziano model (Ref. 2) is a particular example of this scheme. The on-mass-shell appearance of the Adler zero is ensured by setting  $\alpha_\rho(1) = \frac{1}{2}$ , and the scale is determined by the residue of the  $\rho$  pole; this means that the  $s$ - and  $p$ -wave scattering lengths in this model must be close to those given by Weinberg and by the data, which of course they are.

PHYSICAL REVIEW D

VOLUME 7, NUMBER 5

1 MARCH 1973

## Nuclear Reactions at High Energy\*

George W. Barry

*Department of Physics, Purdue University, West Lafayette, Indiana 47907*

(Received 16 October 1972)

In the quark model, nuclei ( $B \leq 2$ ) have exotic quantum numbers. Given a nuclear reaction in which certain quantum numbers are exchanged, what is the scattering amplitude at high energies, in the GeV region? Does it have Regge behavior? Is it dual? Are there multi-baryon resonances? In this context we present a general survey of all high-energy nuclear reactions—mainly those involving light nuclei. For  $B = 0$  exchange reactions, like  $\pi d \rightarrow \pi d$  and  $\pi^- h \rightarrow \pi^0 t$  ( $h \equiv {}^3\text{He}$ ,  $t \equiv {}^3\text{H}$ ), there is the impulse and rescattering (Glauber) model. For  $B = 1$  exchange we discuss the one-pion-exchange (OPE) model for  $pp \rightarrow d\pi^+$ ,  $pd \rightarrow ap$ , and  $\gamma d \rightarrow pn$ , and the “knock-on” model for  $pd \rightarrow \pi^+ t$ ,  $dd \rightarrow tp$ ,  $dh \rightarrow hd$ ,  $\gamma h \rightarrow pd$ , and  $\gamma\alpha \rightarrow pt$ . In the case of  $B = 2$  exchange we examine the impulse and rescattering diagrams for  $\pi d \rightarrow d\pi$ ,  $\gamma d \rightarrow d\pi^0$ , and  $\gamma d \rightarrow d\gamma$ , and use the OPE model to calculate cross sections for  $pd \rightarrow t\pi$ ,  $pt \rightarrow tp$ , and  $ph \rightarrow hp$ . Briefly considered are: (1) backward elastic scattering from heavy nuclei ( $pA \rightarrow Ap$ ) and (2) inclusive nuclear reactions such as  ${}^{14}\text{N} + A \rightarrow {}^6\text{Li} + \text{anything}$  and  $pA \rightarrow \bar{d} + \text{anything}$ . We postulate that in general nuclear reactions have Regge behavior, but are not dual, because so far there are no exotic multibaryon resonances. Nuclear reactions appear to be completely dominated by anomalous singularities, whereas ordinary nonexotic hadron reactions appear to be dominated by normal singularities and poles.

### I. INTRODUCTION

Given a two-body nuclear reaction in which certain quantum numbers are exchanged, what is the differential cross section at high energy, in the GeV region? Forward diffraction scattering has received the lion's share of the attention because the cross sections are large and do not fall off with energy. In this paper, we will be concerned mainly with nondiffractive reactions, those in which quantum numbers are exchanged.

Nuclei are weakly bound systems of protons and neutrons. What is remarkable is that the nucleons retain their identities and do not melt into a multi-baryon state bearing no resemblance to its constituents. The general expectation is that nuclear reactions should be completely accountable in

terms of the more fundamental nucleon-nucleon interactions. The specific mechanisms are believed to be very complicated and not really worth investigating.

At asymptotic energies the problem might simplify. Let us assume that the scattering amplitude has Regge behavior at high energy. Recall that Regge poles were first introduced into hadron physics as a general prescription for ensuring that unitary bounds on scattering amplitudes are not violated. If only a spin- $J \geq 2$  object is exchanged, the cross section will grow with energy, and thereby violate the Froissart bound. Most of this contribution must therefore be canceled by other high-spin exchanges, and the Regge prescription is the simplest way of ensuring this.

The  $p$ - $n$  channel has a bound state, the deuteron.

There are no known excited states of the deuteron, and above the  $p$ - $n$  threshold no genuine dibaryon resonances have yet been seen. One of the nucleons comprising the deuteron can be excited into a resonance, but the total dibaryon system is not an eigenstate of spin and parity. Except for the deuteron, the channel appears to be empty.

If nuclear reactions have Regge behavior (at least for nonexotic exchange), and the direct channel has no true resonances, then nuclear reactions cannot be dual in the same sense as ordinary hadron ( $B \leq 1$ ) reactions.

The most interesting characteristic of nuclei is that they have "exotic" quantum numbers. (However, they are not the exotic states predicted by duality diagrams, such as in  $B\bar{B} - B\bar{B}$ .<sup>1</sup>) The exotic classification derives from the quark model. Any hadron which cannot be constructed from  $qqq$  or  $\bar{q}q$  is defined to be exotic. The quark model tells us nothing about nuclear forces, because they are not quark-quark forces. So it should not be too surprising if nuclear reactions are not dual.

Consider now a reaction in which the quantum numbers of the deuteron are exchanged. At low energies the momentum transfer is close to the deuteron pole, and so it should dominate the amplitude. At high energies, the momentum transfer goes to zero, and deuteron exchange should no longer be a valid description. Is the leading  $t$ -channel singularity a deuteron Regge trajectory? But, except for the deuteron, this channel appears to be empty. Is it valid to extrapolate a deuteron trajectory, obtained from a potential description near the deuteron pole at  $t=4 \text{ GeV}^2$ , all the way over to  $t=0$ ? Even if one could make such an extrapolation, the trajectory would probably be highly curved and have a very low intercept. A  $\Delta \otimes \Delta$  or  $N_\alpha \otimes N_\alpha$  Regge cut is likely to be the leading  $t$ -

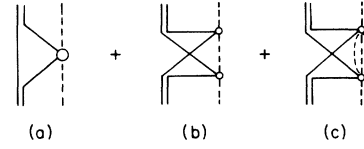


FIG. 1.  $\pi d \rightarrow \pi d$ : (a) Impulse, (b) elastic rescattering, and (c) inelastic rescattering diagrams.

channel singularity which determines the high-energy behavior.

The only way these fundamental questions are going to be answered is by investigating high-energy nuclear reactions where the cross sections are small and falling rapidly with energy. In I we examined the simplest  $B=1$  exchange reactions; namely,  $pp - d\pi^+$ ,  $pp - d\rho^+$ , and  $pd - dp$ . In this paper we present a general overview of all nuclear reactions, concentrating mainly on those involving only light nuclei. With heavy nuclei the basic mechanism is likely to be obscured by multiple-scattering effects. Also, isospin will be badly broken by the large Coulomb fields.

In analyzing the various nuclear reactions we will assume that nuclei are simply composite states of protons and neutrons, and nothing more. This provides us with a fairly well-defined prescription for computing cross sections which can be compared with experimental data. Our program is to extend this simple picture to high-energy, high-momentum-transfer, and large-baryon-number-exchange reactions, where the cross sections are likely to be very small. Our predictions may prove wrong, but at least we will be able to spot any gross discrepancy, signaling, for example, the production of a multibaryon resonance. This is not so far-fetched, since, after all, exoticity has not prevented nuclei from existing.

## II. $B=0$ EXCHANGE

The simplest nuclear reaction is  $\pi d \rightarrow \pi d$ . The impulse and elastic-rescattering diagrams in Figs. 1(a) and 1(b) can give an accurate account of the scattering amplitude near the forward direction.<sup>2</sup> Neglecting spin, isospin, and the  $D$ -wave component of the deuteron wave function, a relativistic treatment leads to the following relation between the  $\pi$ - $d$  and  $\pi$ - $N$  scattering amplitudes<sup>3,4</sup>:

$$T_{\pi d}(s_{\pi d}, t) \approx 2G_d(-\frac{1}{4}t) [T_{\pi p}(s_{\pi N}, t) + T_{\pi n}(s_{\pi N}, t)] \\ + \frac{i}{4\pi^2 M_d k_L} \int d^2p G_d(\vec{p}^2) T_{\pi p}(s_{\pi N}, \frac{1}{4}t + \vec{p}^2 - \vec{d} \cdot \vec{p}) T_{\pi n}(s_{\pi N}, \frac{1}{4}t + \vec{p}^2 + \vec{d} \cdot \vec{p}), \quad (2.1)$$

where  $t = -\vec{d}^2$  and

$$k_L^2 = \left( \frac{s_{\pi d} - u_{\pi d}}{4 M_d} \right)^2 \left( 1 - \frac{t}{4 M_d^2} \right)^{-1} - \mu^2 \left( 1 - \frac{t}{4 \mu^2} \right). \quad (2.2)$$

In terms of the deuteron wave function the form factor is

$$\begin{aligned} G_d(q^2) &= \int d^3x e^{-i\mathbf{q}\cdot\mathbf{x}} |\psi_d(x)|^2 \\ &= \int d^3p \phi_d^*(\vec{p} - \frac{1}{2}\vec{q}) \phi_d(\vec{p} + \frac{1}{2}\vec{q}). \end{aligned} \quad (2.3)$$

The scattering amplitude is normalized such that for spinless particles the center-of-mass differential cross section is

$$\frac{d\sigma}{d\Omega} = \frac{|T|^2}{64\pi^2 s}. \quad (2.4)$$

The energies in the  $\pi$ - $d$  and the  $\pi$ - $N$  systems are related by

$$s_{\pi d} = 2s_{\pi N} + 2m^2 - \mu^2, \quad (2.5)$$

which simply follows from setting the nucleon energy-momentum equal to half that of the deuteron.

The optical theorem applied to (2.1) gives<sup>5</sup>

$$\sigma_{\pi d} = \sigma_{\pi p} + \sigma_{\pi n} - \frac{\langle r^{-2} \rangle}{4\pi} \sigma_{\pi n} \sigma_{\pi p}, \quad (2.6)$$

where

$$\langle r^{-2} \rangle = \frac{1}{2\pi} \int d^2p G_d(p^2). \quad (2.7)$$

The last term in (2.6) can be interpreted as the geometric shadowing of one nucleon by the other. As the binding energy goes to zero, so does  $\langle r^{-2} \rangle$ , in which case the impulse approximation [Fig. 1(a)] becomes *exact*.

Ignoring the shadow term in (2.6) we see that at high energies  $\sigma_{\pi d}$  goes as  $a + bs^{-1/2}$ . The two terms correspond to Pomanchukon and  $f$ -trajectory exchange (the deuteron is isoscalar). In the resonance region there are prominent bumps, which, of course, are not genuine dibaryon resonances, but are merely due to resonance excitation of one of the nucleons in the deuteron. The  $N^*$  and the spectator nucleon are not in an eigenstate of spin and parity. Although the bumps look like they are due to poles on the second sheet, they are really *short cuts*, that is,  $N^*$  poles which are smeared out by the Fermi momentum.

A clean way of distinguishing between a pole and a short cut is to note that the energy relation (2.5) depends on the meson mass. The bumps should be at different c.m. energies in  $\rho$ - $d$  scattering.

The most important feature of the  $\pi d \rightarrow \pi d$  amplitude is that it is not dual. It has Regge behavior at high energy, but there are no real resonances in the direct channel. The amplitude still satisfies a finite-energy sum rule, in that an extrapolation of the high-energy behavior gives an average description of the bumps in the resonance region.

Quark concepts such as exchange degeneracy are irrelevant for nuclear reactions. For instance, in  $\pi d \rightarrow \pi d$ ,  $s$ -channel exoticity would imply that the residue of the  $f$  trajectory is zero, which, of course, is false. The root of the failure is that nuclei should not even exist in the quark model.

The  $\pi d \rightarrow \pi d$  amplitude is not dual, because in the impulse approximation the amplitude is dominated by a  $t$ -channel anomalous threshold at

$$t = 16\alpha^2 = 16m\epsilon_d \quad (2.8)$$

( $\epsilon_d = 2.224$  MeV is the deuteron binding energy), which is closer to the physical region than is the normal threshold at  $t = 4\mu^2$ .

In general, anomalous singularities preclude duality. But they are not unique to nuclear reactions, they occur whenever the mass ratios are just right. The impulse diagram dominates  $\pi d \rightarrow \pi d$  because the contributions from other singularities are already included or are simply small. The impulse term is remarkably complete, and in adding corrections to it one must be careful not to double count.<sup>6</sup>

Although Figs. 1(a) and 1(b) give a remarkably accurate account of the  $\pi d \rightarrow \pi d$  data, we expect small but significant contributions from inelastic-rescattering diagrams such as Fig. 1(c). It is reasonable to expect that the diagrams in Fig. 1 give a *complete* account of the  $\pi d \rightarrow \pi d$  amplitude, since (in the absence of dibaryon resonances) it is difficult to draw any important diagrams which are not already included.

Nondiffractive reactions such as  $\gamma d \rightarrow \pi^0 d$  and  $\pi^- h \rightarrow \pi^0 t$  (where  $h \equiv {}^3\text{He}$  and  $t \equiv {}^3\text{H}$ ) should also be accountable in terms of impulse and rescattering diagrams, such as in Fig. 1. The meager data support this.<sup>7,8</sup>

One can also look at double-charge-exchange reactions such as  $\pi^-({}^{58}\text{Ni}) \rightarrow \pi^+({}^{58}\text{Fe})$ . Only reactions in which the final nucleus breaks up have been detected so far. One possible mechanism is a double-scattering diagram like Fig. 1(b). For recent reviews see Refs. 8-10.

### III. $B=1$ EXCHANGE

A detailed analysis of  $pp \rightarrow d\pi^+$ ,  $pp \rightarrow d\rho^+$ , and  $pd \rightarrow dp$  was presented in I, so here we will simply review the main results and make some refinements.

A.  $pp \rightarrow d\pi, d\rho$ 

These reactions are best described in terms of the one-pion-exchange (OPE) triangle diagram<sup>11</sup> in Fig. 2(a). The OPE model leads to the following expression relating the  $pp \rightarrow d\pi$  and  $\pi N \rightarrow N\pi$  c.m. differential cross sections:

$$\frac{d\sigma^{pp \rightarrow d\pi}}{d\Omega_\theta} = \frac{1}{2} G_{pd}^2(u) \frac{|d|}{|p|} \frac{s_{\pi N}}{s_{\pi d}} \left( 3 \frac{d\sigma^{\pi^+ p \rightarrow \pi^+ p}}{d\Omega_\delta} - \frac{d\sigma^{\pi^- p \rightarrow \pi^- p}}{d\Omega_\delta} + 3 \frac{d\sigma^{\pi^- p \rightarrow \pi^0}}{d\Omega_\delta} \right) + (\cos\theta \leftrightarrow -\cos\theta) + \text{interference terms}, \quad (3.1)$$

where  $s_{\pi d}$  and  $s_{\pi N}$  are again related by (2.5), and the  $pp \rightarrow d\pi$  and  $\pi N \rightarrow N\pi$  scattering amplitudes have the same squared momentum transfer  $u$ . The forward-backward symmetry of  $pp \rightarrow d\pi$  is because the initial protons are identical. The exchanged pion ( $k_1$ ) is off the mass shell, with mass given by

$$k_1^2 = \frac{1}{2}(m^2 - u). \quad (3.2)$$

The  $\pi N \rightarrow N\pi$  amplitude is assumed to be slowly varying in  $k_1^2$  at fixed  $s_{\pi N}$  and  $\cos\delta$  ( $\cos\delta$ -fixed prescription).

The form factor  $G_{pd}$  is defined in analogy with  $G_d$  in (2.3). In I we obtained

$$G_{pd}(u) = \frac{1}{2} \zeta \alpha \left[ \frac{\alpha}{2\pi(1 - r_t \alpha)} \right]^{1/2} \frac{GF(k_1^2)}{(k_1^2 + \mu^2)} \left( \frac{3k_1^2}{2m} \right)^{1/2}, \quad (3.3)$$

where  $r_t = 1.75$  F,  $G^2/4\pi = 14.7$ ,  $\alpha = (m\epsilon_d)^{1/2} = 45.7$  MeV is the deuteron Fermi momentum, and

$$F(k_1^2) = \left( 1 + \frac{k_1^2 + \mu^2}{60\mu^2} \right)^{-1} \quad (3.4)$$

is the Ferrari-Selleri<sup>12</sup> form factor for the  $\pi NN$  vertex. The OPE coupling strength  $\zeta$  is a dimensionless parameter characterizing the short-distance structure of the deuteron wave function.

An equivalent expression for the form factor is<sup>13</sup>

$$G_{pd}(u) = \sqrt{2} \psi_d(0) \frac{GF(k_1^2)}{(k_1^2 + \mu^2)} \left( \frac{3k_1^2}{2m} \right)^{1/2}, \quad (3.5)$$

which follows straightforwardly in the fashion of (3.17)–(3.19) below. Note that the OPE contribution vanishes when  $\psi_d(0) = 0$ , and not just when  $\epsilon_d = 0$ . A Hulthén wave function gives  $\zeta = 12$ , which is

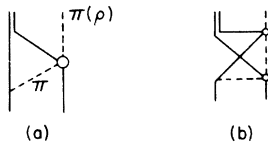


FIG. 2. (a) OPE diagram for  $pp \rightarrow d\pi$  ( $pp \rightarrow d\rho$ ); (b) a possible rescattering contribution analogous to Fig. 1(b). To get the full amplitude, the initial protons must be antisymmetrized.

considerably larger than the value ( $\zeta = 2.9$ ) needed to fit the data.

Theory and experiment<sup>14</sup> are compared in Fig. 3. The bumps in  $pp \rightarrow d\pi$  are due to  $\Delta$  excitation at the  $\pi N \rightarrow N\pi$  vertex, and their energies are correctly predicted by (2.5).  $N^*$  excitation is suppressed because the exchanged meson has  $l = 1$ .<sup>15</sup>

We have calculated the interference term in (3.1) from the  $\pi$ - $N$  phase shifts, and have obtained predictions for  $pp \rightarrow d\pi$  over the entire solid angle and at all energies. The results are terrible, as far as the angular distributions are concerned. On the other hand, the model is very simple, and it does give a decent over-all description of the forward-scattering data at all energies. A formula similar to (3.1) also gives a fair description of  $pp \rightarrow d\rho$  data,<sup>16–18</sup> which are mostly at high energies.

Even in  $\pi d \rightarrow \pi d$  the impulse diagram [Fig. 1(a)] does not by itself give a perfect fit to the data. The rescattering diagram [Fig. 1(b)] is quite im-

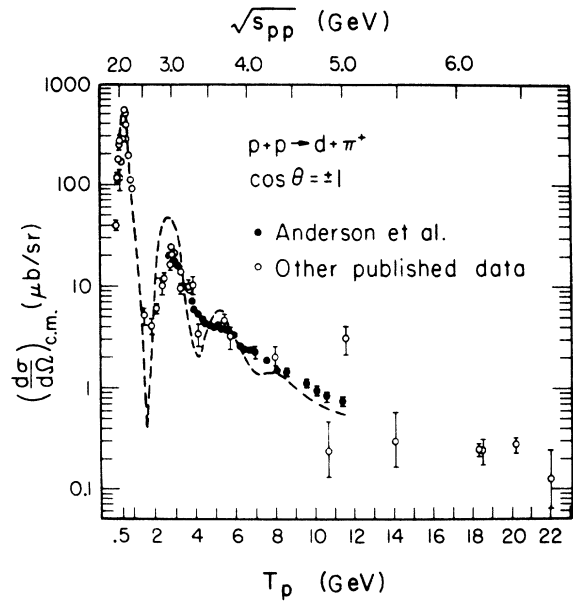


FIG. 3. The center-of-mass forward differential cross section for  $pp \rightarrow d\pi$  as a function of the incident proton kinetic energy in the lab (adapted from Ref. 14). The dashed curve is the OPE prediction from (3.1), ignoring the interference terms.

portant, particularly in the resonance region and at large angles. Correspondingly, in  $pp \rightarrow d\pi$  we can expect a rescattering diagram [Fig. 2(b)] to be important in the resonance region, where the  $\pi N \rightarrow \pi N$  cross section is large.

It has been argued<sup>19-21</sup> that, because the  $pp \rightarrow d\pi$  cross section in the 3-3 resonance region is close to the unitary bound, there must occur a *genuine* dibaryon resonance, a bound  $S$  state of  $N-\Delta$ , which couples weakly to the  ${}^1D_2$  wave of  $p-p$ . The following are criticisms of this interpretation: (i) The experimental angular distribution differs significantly from the expected  $(1 + 3 \cos^2 \theta)$ .<sup>22</sup> (ii)  $\pi d \rightarrow \pi d$  is also large in the 3-3 resonance region, but it is due to a short cut rather than a pole. (iii) Unitarity cannot be relied on to drive the higher  $\Delta$  excitations resonant.

### B. $pd \rightarrow dp$

Using only  $t$ -channel factorization the OPE model can also be applied to  $pd \rightarrow dp$  [Fig. 4(a)], giving<sup>1,13,23</sup>

$$\frac{d\sigma^{pd \rightarrow dp}}{d\Omega_\theta} = G_{pd}^2(u) \frac{|p|}{|d|} \frac{s_{\pi d}}{s_{pd}} \frac{3}{2} \frac{d\sigma^{pp \rightarrow d\pi}}{d\Omega_\delta}, \quad (3.6)$$

where

$$s_{pd} = 2s_{\pi d} + m^2. \quad (3.7)$$

This relation is simpler than (3.1), because there are no interference or crossed terms. Most of the  $p-d$  backward scattering data<sup>22,24</sup> are in the 3-3 resonance region, where the OPE relation (3.6) affords a good fit. We expect that rescattering contributions, which are important in  $pp \rightarrow \pi d$ , are small for  $pd \rightarrow dp$ , because  $NN \rightarrow NN$  does not have any prominent resonances.

At low energies the momentum transfer  $u$  is close to the nucleon pole, which therefore dominates the amplitude. This is the familiar one-nucleon-exchange (ONE) mechanism responsible for the deuteron-stripping reactions in nuclear physics. With increasing energy  $u_{\min}$  goes from  $m^2$  to zero, and we would expect a Regge description involving all the resonances on the  $N_\alpha$  trajectory to be more appropriate. As can be seen from Fig. 4(b), the OPE triangle serves as the  $d-p-N_\alpha$  residue.

The ONE diagram should not be added to the OPE diagram [Fig. 4(a)], because they both contain Fig. 4(b). They merely differ in how the interaction bubble is drawn. At low energies, ONE is an accurate approximation, whereas above, say, the threshold for pion production, OPE is more appropriate.

The OPE diagram for  $pd \rightarrow dp$  already contains much of the rescattering diagram, such as Fig.

1(b), and the two contributions should not be added.<sup>23</sup> Fortunately, the impulse and the elastic-rescattering diagrams are too small to account for the  $pd \rightarrow dp$  backward peak.<sup>25</sup>

The OPE triangle diagrams in Figs. 2(a) and 4(a) have an anomalous threshold at<sup>26-29</sup>

$$u \approx m^2 + 2\mu(\mu + 2\alpha), \quad (3.8)$$

which is below the normal threshold at  $(m + \mu)^2$ . The nucleon pole at  $u = m^2$  should not be counted, because it is already contained in the  $\pi N \rightarrow N\pi$  scattering vertex.

### C. Polarization

The OPE model predicts that the polarization in  $pd \rightarrow dp$  (with the initial proton polarized) should be the same as in  $pp \rightarrow d\pi$ , at the corresponding angle and energy. At 425 MeV the polarization in  $pd \rightarrow dp$  (Ref. 30) was found to be substantially larger than in  $pp \rightarrow d\pi$ .<sup>31</sup> The discrepancy might be because the energy is too low. ONE or Glauber scattering extended to the backward direction is likely to give a more accurate description of  $pd \rightarrow dp$  at low energies.

Another test<sup>32</sup> is to relate the  $\rho$  polarizations in  $pp \rightarrow d\rho$  and  $\pi N \rightarrow N\rho$ . If we can safely ignore the interference term in (3.1), the OPE prediction follows from the replacement

$$\frac{d\sigma}{d\Omega} \rightarrow \rho_{\lambda\lambda'} \frac{d\sigma}{d\Omega}. \quad (3.9)$$

The  $\rho$ -spin density matrices can be easily determined from the  $\rho \rightarrow \pi\pi$  decay distributions. But in order to relate the  $pp \rightarrow d\rho$  and  $\pi N \rightarrow N\rho$  density matrices, the  $\pi N \rightarrow N\rho$  cross sections must also be measured. Also, there is the ambiguity of choosing a frame in which the  $\pi N \rightarrow N\rho$  density matrices are slowly varying when the pion goes off the mass shell.

Polarization measurements may eventually provide important tests of the OPE model, but they have the drawback that the polarization is kinematically zero at  $0^\circ$  and  $180^\circ$ , where the model is most reliable.

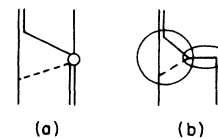


FIG. 4. (a) OPE diagram for  $pd \rightarrow dp$ . This already includes the ONE diagram (b). How the interaction bubble is drawn determines what picture is emphasized.

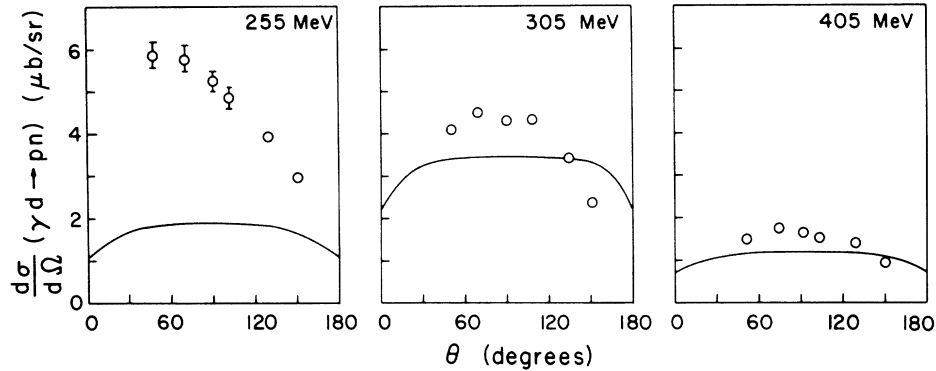


FIG. 5. The c.m. differential cross section for  $\gamma d \rightarrow pn$ . The solid lines are the OPE predictions from (3.10), neglecting the interference terms. The data are from Ref. 33.

#### D. $\gamma d \rightarrow pn$

Although  $\gamma d \rightarrow pn$  cannot be related to a simple linear combination of  $\gamma N \rightarrow N\pi$  cross sections [as in (3.1)], almost all the data are in the 3-3 resonance region where the  $\gamma N \rightarrow N\pi$  amplitude is almost purely  $I = \frac{3}{2}$ . In the 3-3 region the OPE model gives

$$\frac{d\sigma^{\gamma d \rightarrow pn}}{d\Omega_\theta} = G_{pd}^2(u) \frac{|p_n| |p_\gamma| s_{\gamma p}}{|d_\gamma| |p_\pi| s_{\gamma d}} \frac{4}{3} \frac{d\sigma^{\gamma p \rightarrow p\pi^0}}{d\Omega_\delta} + (\cos\theta \rightarrow -\cos\theta) + \text{interference terms}, \quad (3.10)$$

where

$$s_{\gamma d} = 2s_{\gamma p} + 2m^2, \quad (3.11)$$

and  $G_{pd}(u)$  is given by (3.3) with  $\zeta = 2.9$  (the same as for  $\pi d \rightarrow pp$ ).

The forward-backward symmetry of (3.10) is due to the fact that only an isovector photon can produce a 3-3 resonance. In the 3-3 region

$$\frac{d\sigma^{\gamma p \rightarrow p\pi^0}}{d\Omega_\delta} \approx \frac{\sigma_0}{16\pi} (5 - 3 \cos^2\delta), \quad (3.12)$$

and we expect a similar angular distribution for  $\gamma d \rightarrow pn$ . Neglecting the interference term in (3.10), and using the  $\cos\delta$ -fixed prescription to relate  $\theta$  and  $\delta$ , we get the results displayed in Fig. 5.<sup>33</sup> The 3-3 resonance should give a peak at about 300 MeV. The model gives a fair account of the data

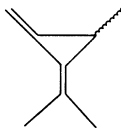


FIG. 6. Deuteron-pole diagram for  $pn \rightarrow d\gamma$ .

above 260 MeV, below which ONE gives a better description.

It is double counting to add the ONE and OPE contributions (as done in Ref. 34). It is also double counting to add the deuteron-pole diagram in Fig. 6, because the pion plays an important role in binding the deuteron.

#### E. $K^- d \rightarrow \Lambda N, \Sigma N$

There are no data on these processes. For the OPE predictions see Ref. 35.

#### F. $\pi^- d \rightarrow p\Delta^-$

This reaction, in which the quantum numbers of the  $\Delta^{++}$  are exchanged, has been proposed as a probe of the  $\Delta$ - $\Delta$  content of the deuteron wave function.<sup>36</sup> The problem is that the OPE contribution [Fig. 7(a)] has to be picked out, by means of the missing mass, from the large background coming from deuteron breakup [Fig. 7(b)]. In fact, Fig. 7(a) is really a final-state-interaction correction to Fig. 7(b).

It is important to note that the triangle diagram [Fig. 7(a)] has no  $u$ -channel anomalous singularity. Even if it did, it would be canceled by the same singularity in Fig. 7(b).<sup>37</sup> The only anomalous singularity comes from Fig. 7(c), and is very far away. It would be very surprising if the  $\pi^- d \rightarrow p\Delta^-$  differential cross section were not extremely small.

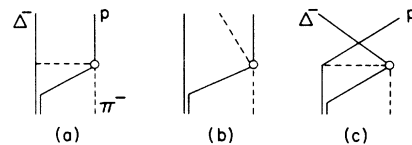


FIG. 7.  $\pi^- d \rightarrow p\Delta^-$ : (a) OPE, (b) background, and (c) exchange diagrams.

G.  $pd \rightarrow \pi t$ 

A natural ansatz is the OPE diagram in Fig. 8(a). The energies in  $pd \rightarrow \pi t$  and  $\pi N \rightarrow N\pi$  are related by

$$s_{\pi t} = 3s_{\pi N} + 6m^2 - 2\mu^2. \quad (3.13)$$

Unfortunately, the two spectator nucleons must be in an unbound  $I=1$  state. This diagram should give a contribution proportional to the  $I=\frac{1}{2}$  exchange  $\pi N \rightarrow N\pi$  cross section ( $3\sigma^+ - \sigma^- + 3\sigma^0$ ), but it is very hard to estimate the value of the off-shell  $\pi-d$  ( $pp$ ) vertex. In order to get a deuteron spectator, an isoscalar meson would have to be exchanged.

Another contribution comes from the "knock-on" diagram in Fig. 8(b).<sup>38-40</sup> The diagram in Fig. 8(c) is likely to be relatively unimportant. This can be checked by seeing whether, say,  $^{13}\text{C}(p, \pi^-)^{14}\text{O}$  is suppressed relative to  $^{13}\text{C}(p, \pi^+)^{14}\text{C}$ . Recent data<sup>41</sup> indicate that  $(p, \pi^-)$  is generally suppressed by a factor 100-200.

In the literature<sup>38-40</sup> the knock-on contribution has been calculated only nonrelativistically. Since the process is inelastic, this is probably inappropriate at high energies. In the following we present a relativistic treatment similar to that for  $\pi d \rightarrow \pi d$ .<sup>3,4</sup>

The amplitude corresponding to the diagram in Fig. 8(b) is (neglecting spin)

$$\int \frac{d^4n}{(2\pi)^4} \frac{\Phi_d(p_1^2, n^2) T^{pp \rightarrow d\pi}(s_{\pi d}, u, p_1^2, d_1^2) \Phi_t(d_1^2, n^2)}{(p_1^2 + m^2 - i\epsilon)(n^2 + m^2 - i\epsilon)(d_1^2 + M_d^2 - i\epsilon)}, \quad (3.14)$$

where  $\Phi_d$  and  $\Phi_t$  are the  $d$ - $p$ - $n$  and  $t$ - $d$ - $n$  vertex functions, respectively. The impulse approximation corresponds to putting the spectator neutron on the mass shell by means of the prescription

$$\begin{aligned} & (n^2 + m^2 - i\epsilon)^{-1} \rightarrow 2\pi i \delta^+(n^2 + m^2) \\ & = \frac{\pi i}{n_0} \delta(n_0 - (\vec{n}^2 + m^2)^{1/2}). \end{aligned} \quad (3.15)$$

This gives

$$\begin{aligned} p_1^2 &= (d-n)^2 \approx -m^2 + 2(\vec{n} - \frac{1}{2}\vec{d})^2 + 2m\epsilon_d, \\ d_1^2 &= (t-n)^2 \approx -M_d^2 + 3(\vec{n} - \frac{1}{3}\vec{t})^2 + 2M_d(\epsilon_t - \epsilon_d). \end{aligned} \quad (3.16)$$

In terms of the wave functions

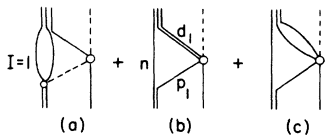


FIG. 8.  $pd \rightarrow \pi t$ : (a) OPE, (b) knock-on, and (c) knock-on with isovector  $NN$  state.

$$\begin{aligned} \frac{1}{(2M_d)^{1/2}} \frac{\Phi_d(p_1^2)}{(p_1^2 + m^2)} &= (2\pi)^{3/2} \phi_d^*(\vec{n} - \frac{1}{2}\vec{d}) \\ &= \int d^3x \psi_d^*(x) \exp[i\vec{x} \cdot (\vec{n} - \frac{1}{2}\vec{d})], \end{aligned} \quad (3.17)$$

$$\begin{aligned} \frac{1}{(2M_t)^{1/2}} \frac{\Phi_t(d_1^2)}{(d_1^2 + M_d^2)} &= (2\pi)^{3/2} \phi_t(\vec{n} - \frac{1}{3}\vec{t}) \\ &= \int d^3x \psi_t(x) \exp[-i\vec{x} \cdot (\vec{n} - \frac{1}{3}\vec{t})], \end{aligned} \quad (3.18)$$

the amplitude (3.14) becomes

$$(M_d M_t)^{1/2} \int \frac{d^3n}{n_0} \phi_d^*(\vec{n} - \frac{1}{2}\vec{d}) \phi_t(\vec{n} - \frac{1}{3}\vec{t}) T^{pp \rightarrow d\pi}(s_{\pi d}, u, \vec{n}), \quad (3.19)$$

which in the peaking approximation leads to

$$T^{p d \rightarrow \pi t}(s_{\pi t}, u) \approx \sqrt{6} G_{dt}(\Delta^2) T^{pp \rightarrow d\pi}(s_{\pi d}, u), \quad (3.20)$$

where

$$G_{dt}(\Delta^2) = \int d^3x e^{-i\Delta \cdot x} \psi_d^*(x) \psi_t(x), \quad (3.21)$$

$$\vec{\Delta} = \frac{1}{2}\vec{d} - \frac{1}{3}\vec{t}. \quad (3.22)$$

Ignoring spin, (3.20) gives the result

$$\frac{d\sigma^{pd \rightarrow \pi t}}{d\Omega_\theta} = 6G_{dt}^2(\Delta^2) \frac{|t_\pi| |p_p| s_{\pi d}}{|d_p| |d_\pi| s_{\pi t}} \frac{d\sigma^{pp \rightarrow d\pi}}{d\Omega_\theta}, \quad (3.23)$$

which differs from that in Refs. 38-40.

The relation between  $s_{\pi t}$  and  $s_{\pi d}$  is determined by the value of  $\vec{n}$  at which  $\phi_d^* \phi_t$  peaks. If the vertex functions  $\Phi_d$  and  $\Phi_t$  are constant, this will occur when

(i) the internal deuteron is on the mass shell ( $\vec{n} \approx \frac{1}{3}\vec{t}$ );

$$d_1^2 + M_d^2 = 0, \quad p_1^2 + m^2 = \frac{1}{3}(m^2 - u), \quad (3.24)$$

$$s_{\pi t} = \frac{3}{2}s_{\pi d} + 3m^2 - \frac{1}{2}\mu^2, \quad (3.25)$$

in which case the 3-3 resonance bump should occur at a proton kinetic energy  $T_p \approx 450$  MeV in  $pd \rightarrow \pi t$ ; or when

(ii) the internal proton is on the mass shell ( $\vec{n} \approx \frac{1}{2}\vec{d}$ );

$$d_1^2 + M_d^2 = \frac{1}{2}(m^2 - u), \quad p_1^2 + m^2 = 0, \quad (3.26)$$

$$s_{\pi t} = 2s_{\pi d} + m^2, \quad (3.27)$$

in which case the resonance bump should be at  $T_p \approx 600$  MeV. The energy relation (3.25) is compatible with (3.13) and (2.5), whereas (3.27) is not.

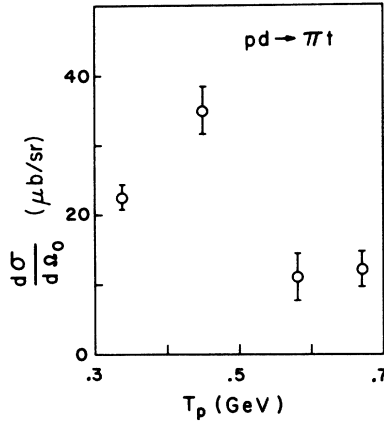


FIG. 9. The c.m. forward differential cross section for  $pd \rightarrow \pi^+ t$  at various proton lab energies. The data are from Refs. 42-47.

In Fig. 9 the  $pd - \pi t$  forward-cross-section data<sup>42-47</sup> peak at about 450 MeV, thus favoring (3.25). This implies that the triton vertex function  $\Phi_t$  falls off more rapidly than  $\Phi_d$ .

Another tricky ambiguity is that  $\bar{\Delta}^2$  is not a relativistic invariant. Two possible prescriptions are to replace  $\bar{\Delta}^2$  by

$$(a) \quad \Delta_a^2 = \bar{\Delta}^2 - \left(\frac{1}{2}d_0 - \frac{1}{3}t_0\right)^2 = \frac{1}{6}(m^2 - u) \quad (3.28)$$

or

$$(b) \quad \Delta_b^2 = \bar{\Delta}^2 - \bar{\Delta}_{\min}^2 = u_{\min} - u. \quad (3.29)$$

The Gaussian wave functions

$$\psi_d(x) = \left(\frac{\beta_d^2}{\pi}\right)^{3/4} \exp\left(-\frac{1}{2}\beta_d^2 x^2\right), \quad (3.30)$$

$$\psi_t(x) = \kappa_t^{1/2} \left(\frac{\beta_t^2}{\pi}\right)^{3/4} \exp\left(-\frac{1}{2}\beta_t^2 x^2\right) \quad (3.31)$$

[where  $\beta_d = 87$  MeV (Ref. 48),  $\beta_t \approx 106$  MeV (Ref. 49)] inserted into (3.21) yield

$$G_{dt}^2(\Delta^2) = \kappa_t \left(\frac{2\beta_d\beta_t}{\beta_d^2 + \beta_t^2}\right)^3 \exp\left(\frac{-\Delta^2}{\beta_d^2 + \beta_t^2}\right). \quad (3.32)$$

$\psi_t(x)$  is the  $d$ - $n$  component of the triton wave function, and  $\kappa_t$  is the total probability that the triton is in such a configuration. If the internucleon correlations can be neglected, then  $\kappa_t = \frac{1}{2}$ , meaning that the triton has an equal probability of being in an  $N-(NN)_{I=1}$  configuration.<sup>49</sup> In obtaining the estimate  $\beta_t \approx 106$  MeV we had to assume that the deuteron radius is much smaller than the triton radius, which is certainly very questionable.

We insert the experimental differential cross sections for  $pd \rightarrow \pi t$  (Refs. 42-47) and  $pp \rightarrow d\pi$  (Ref.

22) into (3.23) and solve for  $G_{dt}^2(\Delta^2)$ . The energies are related by (3.25), and the scattering angles are related by equating the momentum transfers in the two processes ( $u$ -fixed prescription). In Fig. 10, the experimental values for  $G_{dt}^2$  are plotted versus  $\Delta_a^2$  and  $\Delta_b^2$  [defined by (3.28) and (3.29)]. A fit to the form (3.32) gives

$$(a) \quad \kappa_t = 0.7, \quad \beta_t = 115 \text{ MeV},$$

$$(b) \quad \kappa_t = 0.2, \quad \beta_t = 300 \text{ MeV}.$$

Although the variable  $\Delta_b^2$  seems to give a better fit, it entails an unacceptably large value for  $\beta_t$ . [Note Added in Proof. There is an error in Eq. (3.29). The quantity  $u_{\min} - u$  should be divided by 6. Consequently, the fit to the form (3.32) with  $\Delta^2 = \Delta_b^2$  really yields  $\kappa_t = 0.03$  and  $\beta_t = 95$  MeV.]

The diagrams in Fig. 8 have the essential features that they have Regge behavior at high energy and they already contain the ONE pole. Although there clearly seems to be a 3-3 resonance bump at 450 MeV in  $pd - \pi t$ , all three diagrams in Fig. 8 suggest a bump at this energy, and our analysis cannot be considered as proof that Fig. 8(b) is the dominant one.

#### H. $dd \rightarrow tp$ and $dh \rightarrow hd$

We want to relate  $dd - pt$  to  $pd - dp$  using a knock-on diagram like Fig. 8(b). Unfortunately, the initial deuterons are identical and must be symmetrized, giving rise to incalculable interference terms.

No interference term arises in Fig. 11, which relates

$$\frac{d\sigma^{dh \rightarrow hd}}{d\Omega_\phi} = 6G_{dt}^2(\Delta_a^2) \frac{|d_d|}{|t_p|} \frac{s_{dd}}{s_{dh}} \frac{d\sigma^{dd \rightarrow tp}}{d\Omega_\phi}, \quad (3.33)$$

where

$$s_{dh} = \frac{3}{2}s_{dd} + m^2 \quad (3.34)$$

and  $G_{dt}(\Delta_a^2)$  is the same as in (3.23). The scattering angles are related by equating the momentum transfers  $u$ . There are no high-energy data on either  $dd \rightarrow tp$  or  $dh \rightarrow hd$ .

#### I. $\gamma h \rightarrow pd$ and $\gamma\alpha \rightarrow pt$

We expect that the knock-on model (3.23) should also relate  $\gamma h - pd$  to  $\gamma d - pn$ . The  $\gamma h - pd$  cross section at  $90^\circ$  has been measured up to  $E_\gamma = 500$  MeV,<sup>50</sup> and there is no indication of a 3-3 resonance bump expected at around 300 MeV. However, the 3-3 also appears to be washed out in  $\gamma d - pn$ .<sup>50</sup> Perhaps the energy is too low and the angle too large for the model to be applicable. On the other hand, there is a distinct bump in  $\gamma\alpha - pt$  at about 300 MeV for scattering at  $90^\circ$ .<sup>50</sup>



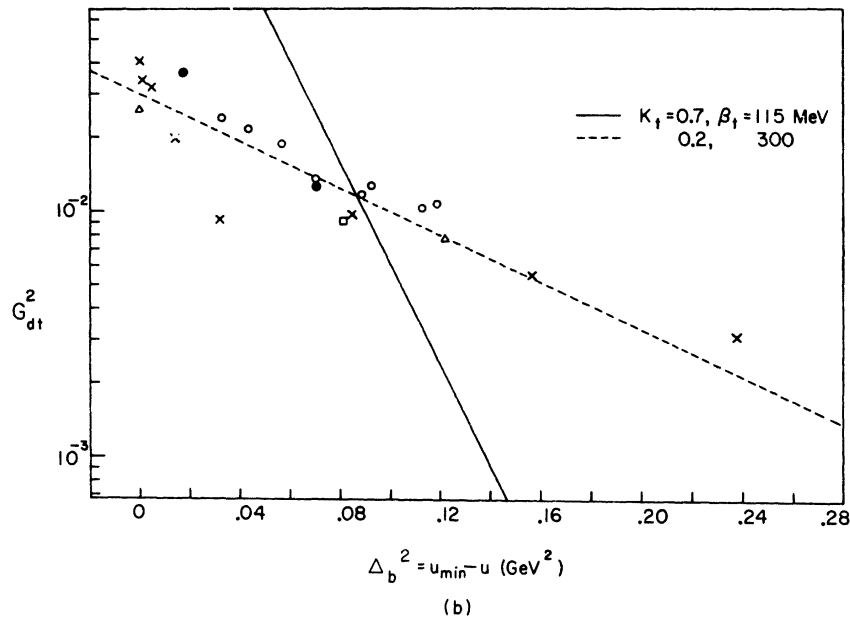
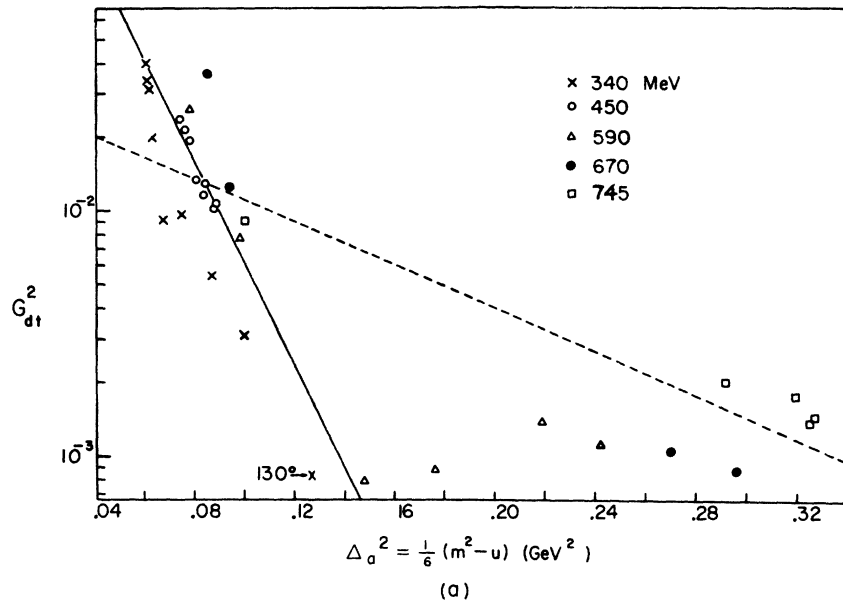


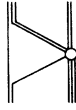
FIG. 10. The form factor  $G_{dt}^2(\Delta^2)$  calculated from (3.23), and the  $pp \rightarrow d\pi$  and  $pd \rightarrow \pi t$  cross-section data (Refs. 22, 42-47) at various proton lab energies. The squared momentum transfer is  $u = -(d-t)^2$ . The lines are fits to the Gaussian form (3.32). (See Note added in proof on p. 1448).

J.  $A(p, \pi^+)A+1$  and  $A(d, p)A+1$

IV.  $B=2$  EXCHANGE

The  $I=\frac{1}{2}$ ,  $B=1$  exchange amplitudes for these processes are related by the knock-on mechanism to  $pp \rightarrow d\pi$  and  $pd \rightarrow d\pi$ , respectively. The model is compatible with the very sparse data on  $A(p, \pi^+)A+1$ , where  $A = {}^3\text{He}$ ,  ${}^4\text{He}$ ,  ${}^{12}\text{C}$ ,  ${}^{13}\text{C}$ ,  ${}^{14}\text{N}$  (Refs. 51 and 52), although rescattering effects are certainly very important.

The only  $B=2$  exchange reaction involving non-exotic hadrons is  $p-\bar{p}$  backward scattering. At 5 GeV/c the differential cross section has a prominent backward peak,<sup>53</sup> which when combined with lower-energy data goes as  $(d\sigma/du)_0 \sim s^{-9.4}$ , corresponding to an effective-trajectory intercept of  $\alpha_{pp}(0) \approx -3.7$ .

FIG. 11. Knock-on diagram for  $dt \rightarrow td$  or  $dh \rightarrow hd$ .A.  $\pi d \rightarrow d\pi$ 

This is the simplest dibaryon-exchange nuclear reaction. In Fig. 12 the experimental backward differential cross section<sup>54-59</sup> is plotted versus the energy. The backward cross section appears to fall off exponentially rather than as a power of the energy. Throughout this energy range,  $\pi d \rightarrow \pi d$  is peaked near the forward direction and flat near  $180^\circ$ .

The most distinctive feature of the data is the bump at 580 MeV.<sup>59</sup> Is it a genuine dibaryon resonance? This is certainly a good place to look for them, since the "background" due to the impulse and rescattering diagrams in Figs. 1(a) and 1(b) is small and falling rapidly with energy.

Up to about 180 MeV, which is the threshold for pion production, it has been demonstrated<sup>60,61</sup> that the impulse and rescattering diagrams can account for the differential cross section data over the entire solid angle. The question is, can this "background" also account for the data above 180 MeV? Progressively refined calculations over the past two decades have shown that simple Glauber scattering<sup>2</sup> gives a surprisingly accurate account of the data all the way out to  $t \approx 2$  GeV<sup>2</sup>. The model works far better than expected.

Consider first the impulse diagram in Fig. 1(a). The c.m. energies of the  $\pi$ - $d$  and  $\pi$ - $N$  systems are related by (2.5); in other words, the incident pion kinetic energy is the same for both targets,

$$T_{\pi}^{(d)} = T_{\pi}^{(N)}, \quad (4.1)$$

irrespective of momentum transfer. In  $\pi N \rightarrow \pi N$  the resonances  $\Delta(1236)$ ,  $N(1520)$ , and  $N(1688)$  occur at  $T_{\pi}^{(N)} = 180$ , 580, and 900 MeV, respectively, which closely correspond to the bump positions in Fig. 12.

It is often argued that (4.1) is true only at  $t=0$ , and that the actual energy relation is momentum-transfer dependent. However, the suggested alternatives have serious defects. For instance, the relation advocated by Alberi and Bertocchi<sup>62</sup> violates energy conservation at the  $d$ - $p$ - $n$  vertex, whereas in a previous work<sup>4</sup> a forceful argument was given for (4.1).

In the impulse diagram, the momentum transfers in  $\pi d \rightarrow \pi d$  and  $\pi N \rightarrow \pi N$  are equal:

$$t_{\pi N} = t_{\pi d} \equiv t. \quad (4.2)$$

The energies in (4.1) are related<sup>4</sup> at the peak value of

$$\phi_d^* \phi_d \propto (p_1^2 + m^2)^{-1} (p_2^2 + m^2)^{-1}, \quad (4.3)$$

which occurs when one of the nucleons of  $\pi N \rightarrow \pi N$  is on the mass shell and the other is off;

$$\begin{aligned} p_1^2 &= (\tfrac{1}{2}d)^2 = -m^2, \\ p_2^2 &= (d' - \tfrac{1}{2}d)^2 = -m^2 - \tfrac{1}{2}t. \end{aligned} \quad (4.4)$$

The amplitude should be symmetrized in  $p_1^2$  and  $p_2^2$ , but this is unnecessary for  $\pi d \rightarrow \pi d$ .

The off-mass-shell  $\pi$ - $N$  amplitude can be related to the physical one by assuming slow off-mass-shell variation at fixed  $t_{\pi N}$  or at fixed  $\cos \theta_{\pi N}$ . With  $t_{\pi N}$  fixed, the angular boundaries do not match up;  $\cos \theta_{\pi d} = -1$  corresponds to  $\cos \theta_{\pi N} < -1$ . Whereas with  $\cos \theta_{\pi N}$  fixed,  $-1 \leq \cos \theta_{\pi N} \leq 1$  maps into  $-1 \leq \cos \theta_{\pi d} \leq 1$ .

At large  $t$  the double-scattering term in Fig. 1(b) should dominate the amplitude, because transferring the momentum in two steps minimizes the form-factor suppression. In the weak-binding limit we may write

$$T_{\pi d}(s_{\pi d}, t) \approx \frac{i}{2\pi M_d k_L} \left\langle \frac{1}{r^2} \right\rangle T_{\pi N}^2(s_{\pi N}, \tfrac{1}{4}t). \quad (4.5)$$

If  $T_{\pi N}$  is taken to be the physical amplitude, with the internal nucleons nearly on the mass shell, then the internal pion must have mass squared

$$m_x^2 \approx \mu^2 - \tfrac{1}{4}t. \quad (4.6)$$

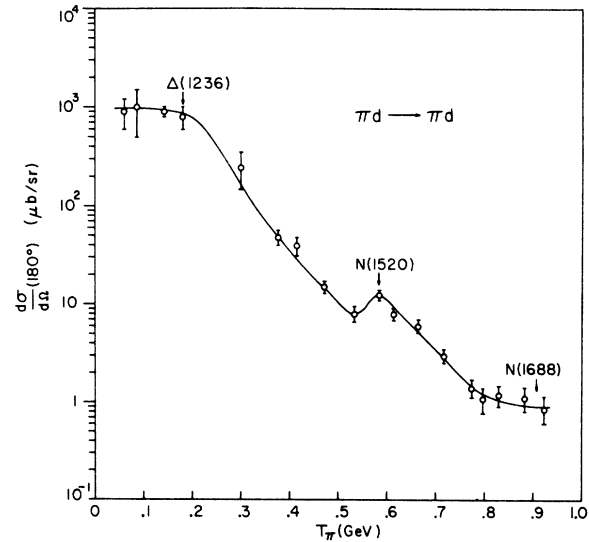


FIG. 12. The  $\pi d \rightarrow \pi d$  c.m. differential cross section at  $180^\circ$  versus the pion kinetic energy in the lab. The data are taken from Refs. 54-59. The curve is simply an eyeball fit. The resonance energies in  $\pi N \rightarrow \pi N$  are indicated.

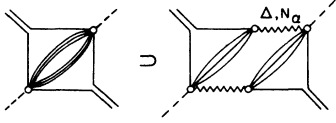


FIG. 13. The inelastic-rescattering diagram for  $\pi d \rightarrow d\pi$  is the same as Fig. 1(c) untwisted, and with the intermediate pions factored into two bunches. This diagram contains a Regge cut.

Near  $t=0$  the diagrams in Figs. 1(a) and 1(b) should give an accurate account of the scattering, but at large momentum transfers the inelastic rescattering diagram in Fig. 1(c) should dominate.

The inelastic rescattering contribution to  $\pi d \rightarrow d\pi$  can be estimated by simply replacing the  $\pi N \rightarrow \pi N$  amplitudes in (4.5) by the amplitudes for  $\pi N \rightarrow N$  + anything. For large  $t$  we estimate

$$\frac{d\sigma^{\pi d \rightarrow \pi d}}{dt} \approx \frac{1}{\pi} \left( \left\langle \frac{1}{r^2} \right\rangle \frac{d\sigma^{\pi N \rightarrow NX}}{d\frac{1}{4}t} \right)^2, \quad (4.7)$$

which like (2.6) also follows from geometrical considerations. It is very difficult to make a more accurate calculation. Fortunately, the multipion intermediate states are unlikely to be terribly important for the energies of interest in Fig. 12.

Barring the existence of dibaryon resonances which couple to nuclei, the diagrams in Fig. 1 should give a complete account of  $\pi d \rightarrow \pi d$  at all angles and energies. The common feature of these diagrams is the energy relation (4.1). More specific predictions are very sensitive to the deuteron wave function at short distances.

What is the asymptotic energy dependence of  $\pi d \rightarrow d\pi$ ? This is hard to measure experimentally, because already at 900 MeV the background due to protons coming from deuteron breakup becomes prohibitive. So far the backward cross section falls off exponentially with energy, but this is unlikely to continue indefinitely. A Regge cut implying a power-law behavior should eventually dominate.

Neither the impulse diagram [Fig. 1(a)] nor the elastic rescattering diagram [Fig. 1(b)] is Regge-behaved in the backward direction. But the inelastic rescattering diagram [Fig. 1(c)] has a  $\Delta \otimes \Delta$  Regge cut, as can be seen in Fig. 13, which is just Fig. 1(c) untwisted and with the multipion intermediate state factored into two bunches. The elastic rescattering diagram does not have a Regge cut

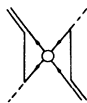


FIG. 14. Triangle diagram relating  $\pi d \rightarrow d\pi$  to  $NN \rightarrow NN$  at high energy.

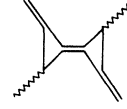


FIG. 15. Deuteron-exchange pole in  $\gamma d \rightarrow d\gamma$ .

because it cannot be so factored.

Asymptotically the  $\pi$ - $d$  backward differential cross section should go as  $s^{2\alpha-1}$ , where  $\alpha = 2\alpha_{\Delta}(0) - 1 = -0.7$ . The  $\Delta \otimes \Delta$  residue may be small, in which case  $N_{\alpha} \otimes \Delta$  or  $N_{\alpha} \otimes N_{\alpha}$  would be the leading cut.

A relation between  $\pi d \rightarrow d\pi$  and  $p\bar{p} \rightarrow \bar{p}p$  is suggested by the triangle diagram in Fig. 14, which has an anomalous threshold at

$$u \approx 4m^2 - (\mu - 2\alpha)^2. \quad (4.8)$$

However, this diagram is already contained in Fig. 13. Nevertheless, the  $\pi$ - $d$  and  $p$ - $\bar{p}$  backward differential cross sections could turn out to be proportional at very high energies.

#### B. $\gamma d \rightarrow d\pi^0$

The  $\gamma d \rightarrow \pi^0 d$  differential cross section at  $180^\circ$  has been measured between 200 and 300 MeV.<sup>63</sup> The impulse and elastic rescattering diagrams imply a 3-3 resonance bump at about 300 MeV. The bump in  $\gamma d \rightarrow d\pi^0$  appears to be centered around 250 MeV.

#### C. $\gamma d \rightarrow d\gamma$

In contrast with  $\pi d \rightarrow d\pi$ , both  $I=0$  and  $I=1$  can be exchanged. The  $I=0$  part has a deuteron-exchange pole (Fig. 15). At low energies the deuteron pole is certainly important, but will it also be important at high energies? Can the deuteron Regge trajectory obtained from potential scattering be extrapolated all the way over to  $u=0$ ? Even if it could, would a Regge cut dominate?

We have postulated that diagrams such as Fig. 1 can give a complete account of the scattering. The deuteron pole is produced by meson-exchange forces, and these are already included in Fig. 13. It would be double counting to simply add Figs. 13 and 15. In other words, the deuteron pole is somehow related to the  $\Delta \otimes \Delta$  (or  $N_{\alpha} \otimes N_{\alpha}$ ) Regge cut.

#### D. $pd \rightarrow t\pi$

The knock-on diagram [Fig. 16(a)] cannot account for the backward-scattering data ( $\Delta_a^2 > 0.12 \text{ GeV}^2$ ) in Fig. 10(a). Therefore, some other mechanism must be responsible for the backward scattering.

The OPE diagram in Fig. 16(b) leads to the relation

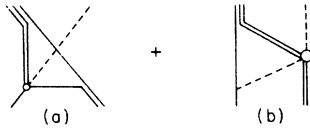


FIG. 16.  $pd \rightarrow t\pi^+$ : (a) Knock-on diagram for  $pd \rightarrow \pi t$  [Fig. 8(b)] at  $180^\circ$ ; (b) OPE diagram.

$$\frac{d\sigma^{pd \rightarrow \pi t}}{d\Omega_\theta} = \frac{1}{2} G_{pt}^2(k_1^2) \frac{|t_\pi| s_{\pi d}}{|p_d| s_{\pi t}} \frac{d\sigma^{\pi d \rightarrow \pi t}}{d\Omega_\delta}, \quad (4.9)$$

where

$$s_{\pi t} = \frac{3}{2} s_{\pi d} + 3m^2 - \frac{1}{2}\mu^2, \quad (4.10)$$

$$k_1^2 = \frac{1}{3} [4m^2 + (t-p)^2], \quad (4.11)$$

$$G_{pt}(k_1^2) \approx \psi_t(0) \sqrt{6} \frac{GF(k_1^2)}{(k_1^2 + \mu^2)} \left( \frac{2k_1^2}{2m} \right)^{1/2}. \quad (4.12)$$

The form factor (4.12) was obtained in a fashion similar to (3.5). The  $\sqrt{2}$  factor is due to the fact that the triton has two helicity states. The scattering angles are related via the  $\cos\delta$ -fixed prescription, where  $\cos\theta = -1$  corresponds to  $\cos\delta = -1$ .

In Fig. 17, the predicted  $pd \rightarrow \pi t$  differential cross section at  $180^\circ$  is compared with the data.<sup>42,43,45,47,64</sup> The value of  $\psi_t(0)$  needed to fit the data is a factor of  $\sqrt{10}$  smaller than that suggested by the Gaussian form (3.32) with  $\kappa_t = \frac{1}{2}$  and  $\beta_t = 100$  MeV. The bump predicted at about 1.05 GeV corresponds to the  $N^*(1520)$  (?) bump in  $\pi d \rightarrow d\pi$  (Fig. 12). Near  $180^\circ$ ,  $pd \rightarrow \pi t$  should have a flat angular distribution like  $\pi d \rightarrow \pi d$ .

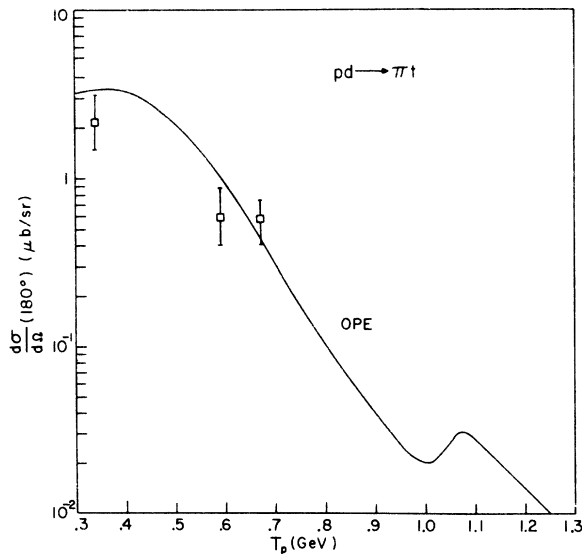


FIG. 17. The c.m. differential cross section for  $pd \rightarrow \pi t$  at  $180^\circ$ . The data are from Refs. 42, 43, 45, 47. The curve is the OPE prediction from (4.9) with the normalization,  $\psi_t(0)$ , chosen to fit the data.

#### E. $pt \rightarrow tp$

The impulse diagrams in Figs. 18(a) and 18(b) do not have Regge behavior near the backward direction, but the OPE diagram in Fig. 18(c) does. Its contribution is given by

$$\frac{d\sigma^{pt \rightarrow tp}}{d\Omega_\theta} = \frac{3}{2} G_{pt}^2(k_1^2) \frac{|p_d| s_{\pi t}}{|t_\pi| s_{pt}} \frac{d\sigma^{pd \rightarrow \pi t}}{d\Omega_\delta}, \quad (4.13)$$

where

$$s_{pt} = \frac{3}{2} s_{\pi t} + \frac{5}{2} m^2, \quad (4.14)$$

$$k_1^2 = \frac{1}{3} (4m^2 - u_{pt}), \quad (4.15)$$

and  $\cos\theta = -1$  corresponds to  $\cos\delta = -1$ . For  $\psi_t(0)$  we use the value needed to fit the  $pd \rightarrow t\pi$  data in Fig. 17. The OPE prediction for  $pt \rightarrow tp$  is plotted in Fig. 19(a). The angular distribution should be flat near the backward direction.

#### F. $ph \rightarrow hp$

Although it is easier to measure,  $ph \rightarrow hp$  is theoretically more complicated than  $pt \rightarrow tp$ , because both  $I=0$  and  $I=1$  can be exchanged. If the  $I=0$  exchange amplitude is small, then isospin invariance implies

$$\frac{d\sigma^{ph \rightarrow hp}}{d\Omega} = \frac{1}{4} \frac{d\sigma^{pt \rightarrow tp}}{d\Omega}. \quad (4.16)$$

The only high-energy datum<sup>65</sup> on  $ph \rightarrow hp$  [Fig. 19(b)] is considerably higher than the OPE prediction from (4.13) and (4.16). The following are possible reasons for the discrepancy:

(i) There may be a large  $I=0$  exchange contribution, such as from the isoscalar-meson-exchange diagram in Fig. 18(d) (which has Regge behavior

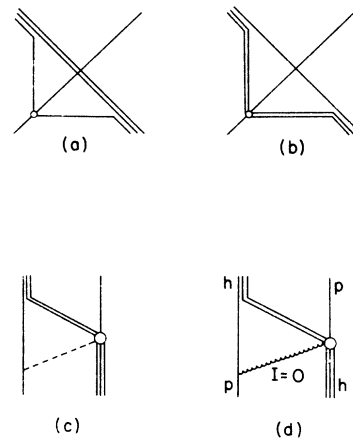


FIG. 18.  $pt \rightarrow tp$  and  $ph \rightarrow hp$ : (a), (b) Impulse diagrams; (c) OPE diagram. The isoscalar-meson-exchange diagram (d) can only contribute to  $ph \rightarrow hp$ .

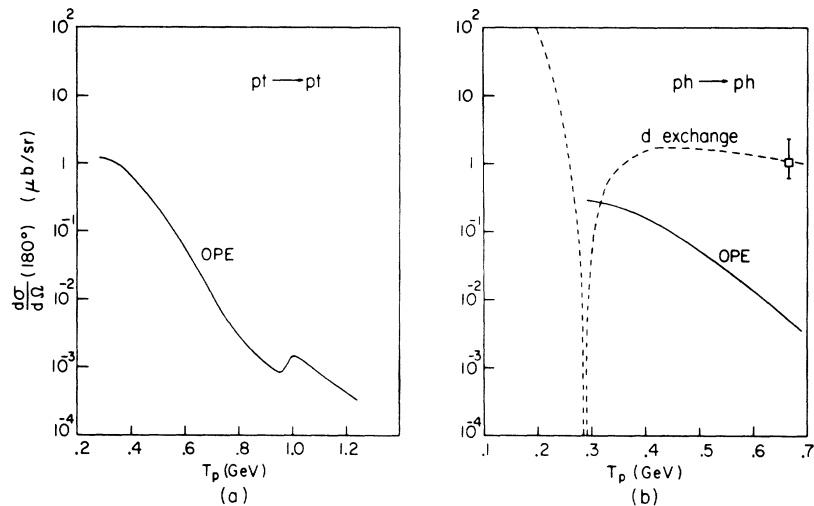


FIG. 19. The (a)  $pt \rightarrow pt$  and (b)  $ph \rightarrow ph$  c.m. differential cross sections at  $180^\circ$ . The OPE predictions are from (4.13) and (4.16), and the estimate of the deuteron-exchange contribution is from Ref. 66. The datum point is from Ref. 65.

at high energy).

(ii) The deuteron-exchange pole may still dominate. The estimate<sup>66</sup> of the  $d$ -pole contribution plotted in Fig. 19(b) is extremely sensitive to the short-distance structure of the helion wave function, which was chosen so as to fit the datum point. The diagram in Fig. 18(d) already contains the  $d$ -exchange pole, but we have no way of evaluating it at this time.

(iii) The OPE model may also fail for  $pt \rightarrow tp$ , in which case the impulse diagrams in Figs. 18(a) and 18(b) (and also rescattering) may still be important. Unfortunately, their contributions are hard to estimate with any confidence. Moreover, Fig. 18(a) is to a large extent already contained in Figs. 18(c) and 18(d).

(iv) Perhaps a  ${}^4\text{Li}$  resonance is being produced, but it is hard to tell from the data.

#### V. $B \geq 3$ EXCHANGE

The world data consist of a few points (Fig. 20) for  $p\alpha \rightarrow \alpha p$  (Ref. 65) and  $p({}^6\text{Li}) \rightarrow ({}^6\text{Li})p$ .<sup>67</sup> So far the backward cross sections fall off rapidly with no sign of any structure. Generally, the falloff is faster the larger the baryon number exchanged.<sup>67</sup>

##### A. Regge Model

Asymptotically,  $pA \rightarrow Ap$  should be dominated by  $\Delta^{(A-1)}$  Regge-cut exchange, implying an energy dependence of  $s^{2\alpha-1}$ , where

$$\begin{aligned} 2\alpha - 1 &= 2(A-1)[\alpha_\Delta(0) - 1] + 1 \\ &= 1 - 1.7(A-1). \end{aligned} \quad (5.1)$$

However, at present energies  $s$  is nearly constant

due to the large mass of the target nucleus. Presumably we should use  $T_p$  instead of  $s$ . Even then, it would be presumptuous to expect this form to fit low-energy data. On the other hand, the Regge form does embody the empirical feature that the power of falloff increases with the baryon number exchanged.

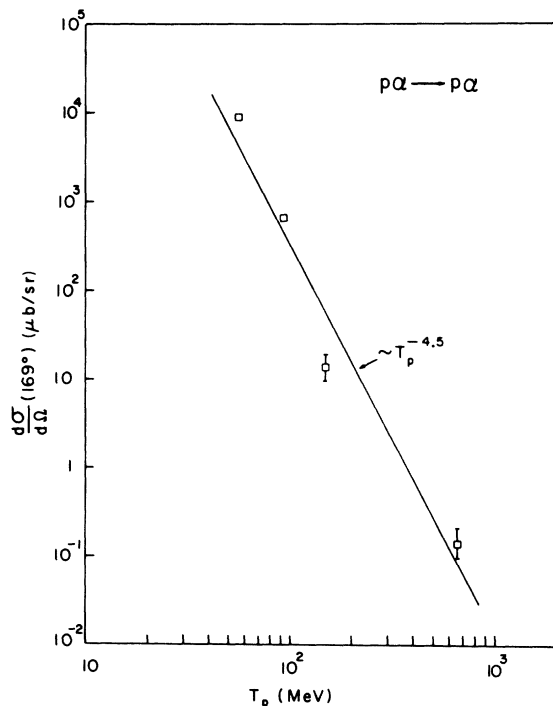


FIG. 20. The c.m. differential cross section for  $p\alpha \rightarrow p\alpha$  at  $169^\circ$ . The high-energy datum is from Ref. 65. The line is simply an eyeball fit.

### B. Impulse Term

How does the impulse contribution, which is proportional to the square of the form factor

$$G_A^{(i)}(q^2) = \int d^3x_1 \cdots d^3x_A e^{iq \cdot x_i} |\psi_A(x_1 \cdots x_A)|^2, \quad (5.2)$$

fall off with momentum transfer? In (5.2) the  $e^{iq \cdot x_i}$  factor averages to zero, except in the region  $|x_i| < |q|^{-1}$ . Consequently we can interpret  $G_A^{(i)}(q^2)$  as the probability of finding the  $i$ th nucleon within a radius  $(-t)^{-1/2}$  of the center of mass of nucleus  $A$ . Since the wave function is unlikely to blow up near  $x=0$ ,<sup>68</sup> we can expect the form factor to fall very rapidly, perhaps exponentially, with momentum transfer.

Previous estimates of  $pA \rightarrow Ap$  at high energy were made by Blokhintsev,<sup>69</sup> who postulated that the backward cross section is proportional to the probability that *all* the nucleons of  $A$  are within a volume  $(-t)^{-3/2}$ . If the wave function is constant near the origin, this leads to a backward cross section falling off as  $T_p^{-1.5(A-1)}$ , which is consistent with the meager data available.<sup>67</sup> However, this model cannot be interpreted in terms of Feynman diagrams, and it is unable to account for the bumpy structure seen in  $pd \rightarrow dp$  and  $\pi d \rightarrow d\pi$ .

### C. Optical Picture

In backward scattering from heavy nuclei, multiple scattering is likely to be very important, in which case an optical formalism would seem most appropriate.

The impact-parameter representation for the scattering amplitude is (neglecting spin)

$$f(s, t) = \int_0^\infty b db J_0(b\sqrt{-t}) a(b, s). \quad (5.3)$$

The differential cross section

$$\frac{d\sigma}{dt} = \pi |f(s, t)|^2 \quad (5.4)$$

falls off rapidly with  $t$  for any reasonable opacity function  $a(b, s)$ . For example, a Gaussian  $a = \exp(-b^2/2R^2)$  gives  $f \sim \exp(\frac{1}{2}R^2 t)$ , while a black disk gives  $f \sim (-t)^{-3/4}$ . The impact-parameter representation has little value for backward scattering because it is very sensitive to the exact form of the opacity function.

In an optical picture, backward scattering is believed to be interpretable in terms of the glory effect<sup>70</sup> encountered in meteorology and in reflecting street signs. It is a classical effect in which the incident wave is internally reflected from the back surface of the target, with c.m. amplitude

$$f \sim k^{-1} J_0(kR \sin(\pi - \theta)). \quad (5.5)$$

Data for 20–50-MeV  $\alpha$  particles scattering off spinless nuclei can be fitted by a Bessel function near the backward direction,<sup>71</sup> but the energy fall-off is much faster than the  $k^{-2}$  predicted by (5.5). Moreover, (5.5) implies a rapidly varying opacity function characteristic of a shiny reflecting surface.<sup>72</sup> It is highly doubtful whether the classical glory effect has any relevance for high-energy backward scattering from “black” nuclear matter.

## VI. INCLUSIVE REACTIONS

As for two-body reactions, we expect inclusive nuclear reactions to involve the impulse approximation, factorization, and Regge behavior, but not duality. Inclusive nuclear reactions promise to be an important source of information about exotic channels. They are the simplest reactions to measure experimentally, and there already exists a wealth of data – so much in fact, that we must defer a more complete account to a future paper. Here we mention a few interesting examples to illustrate the possibilities.

### A. $^{14}\text{N} + A \rightarrow X + \text{anything}$

Fragments ( $X = {}^6\text{Li}$ ,  ${}^{12}\text{C}$ , etc.) are seen which have small momenta in the rest frame of the incident 29-GeV  $^{14}\text{N}$  ions.<sup>73</sup> Also, the momentum spectra and relative abundances of the fragments are independent of the target nucleus  $A = p, {}^{12}\text{C}$ .

To understand these results, consider the impulse diagram in Fig. 21(a), where  $A$  scatters off an  $N-X$  constituent of  $^{14}\text{N}$  without disturbing the spectator  $X$ . The momentum transfer between  $N$  and  $X$  is close to the  $N-X$  pole. Unitarity, the optical theorem, and factorization imply that

$$\sigma(\text{NA} \rightarrow X + \cdots) = \sigma_{\text{tot}}(\text{NA}) \times (\text{probability of finding an } X \text{ cluster in } ^{14}\text{N}), \quad (6.1)$$

which is consistent with the experimental observations.<sup>73</sup>

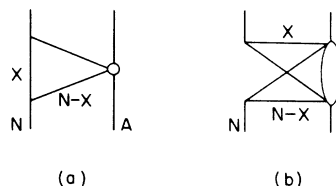


FIG. 21.  $^{14}\text{N} + A \rightarrow ^{14}\text{N} + A$ : (a) Impulse scattering from an  $N-X$  cluster of  $^{14}\text{N}$ ; (b) rescattering from the spectator  $X$ .

The factorization property hinges on  $X$  being a spectator. If the rescattering diagram in Fig. 21(b) contributes substantially to the  $^{14}\text{N}-A$  total cross section, then factorization could break down.

There is some evidence for charge-exchange scattering, where  $X = ^{14}\text{C}, ^{14}\text{O}$ . Significantly, no  $B \geq 15$  fragments are seen, but reactions of this type are most interesting from our point of view.

#### B. $p + A \rightarrow X + \text{anything}$

The inclusive cross sections for  $X = d, p, \pi^+$  production were measured<sup>74</sup> at 6.8 GeV/c for  $X$  emission at 15 mrad and 1.23 GeV/c, which is in the central region and is much larger than the Fermi momentum. The inclusive cross sections  $\sigma^X(\vec{p}) \equiv E d\sigma/d^3p$  go as  $A^\delta$ , where  $\delta_{\pi^+} = 0.45 \pm 0.03$ ,  $\delta_p = 0.69 \pm 0.03$ , and  $\delta_d = 1.24 \pm 0.01$ .

This can be interpreted as follows: Inclusive cross sections are discontinuities, so  $p$  and  $\pi^+$  production should be proportional to the total cross section and go roughly as  $A^{2/3}$ . Since the deuteron is weakly bound,  $\sigma^d(\vec{d})$  should be proportional to the two-particle inclusive cross section  $\sigma^{n,p}(\frac{1}{2}\vec{d}, \frac{1}{2}\vec{d})$ . If the two nucleons are uncorrelated,

$$\sigma^d(\vec{d}) = |f_A|^2 [\sigma^p(\frac{1}{2}\vec{d})]^2 / \sigma_{\text{tot}}(pA). \quad (6.2)$$

This goes as  $A^{4/3}$  if the  $np \rightarrow d$  amplitude,  $f_A$ , is proportional to the time the nucleon pair spends in the nucleus ( $\propto R \propto A^{1/3}$ ).<sup>74</sup>

The data for antideuteron production by high-energy protons<sup>75,76</sup> can be accounted for by<sup>76</sup>

$$\frac{\sigma^{\bar{d}}(\vec{d})}{\sigma^d(\vec{d})} = \left[ \frac{\sigma^{\bar{p}}(\frac{1}{2}\vec{d})}{\sigma^p(\frac{1}{2}\vec{d})} \right]^2. \quad (6.3)$$

Also, the meager data on  $\bar{h}$  production<sup>77</sup> are consistent with

$$\sigma^{\bar{h}}(\vec{h}) \sigma^{\bar{p}}(\frac{1}{3}\vec{h}) \approx [\sigma^{\bar{d}}(\frac{2}{3}\vec{h})]^2. \quad (6.4)$$

It would be very interesting to measure the  $A$  dependences of these inclusive cross sections.

## VII. DISCUSSION

On the basis of our examination of a number of high-energy nuclear reactions, let us abstract a few useful hypotheses which may prove to be of general validity.

1. *Above the multinucleon normal threshold, the  $B \geq 2$  channel is empty of any real resonances.*

2. *Nuclei couple directly only to nucleons.* Specifically, the bare  $d-N-N^*$  coupling should be zero. A  $d-N-N^*$  vertex can be generated from the  $d-p-n$  vertex by a final-state interaction, such as OPE, and adding an  $N-N^*(1688)$  component to the deuteron wave function<sup>78</sup> would run the risk of

double counting. By the same criterion,  $\Delta$  nuclei<sup>79,86</sup> should also be ruled out.

3. *Diagrams with anomalous singularities dominate the scattering amplitude.* This is a precise statement of the tacit assumption usually made when one is interested in calculating a cross section, namely that nuclei are just weakly bound states of nucleons, and nothing more. This is a very strong statement, but as yet there is no clear evidence to contradict it. It implies, for instance, that  $\pi^-d \rightarrow p\Delta^-$  should come only from the backward tail of  $\pi^-d \rightarrow \Delta^-p$  (see Sec. III F).

In contrast, *in the strongly-coupled world of non-exotic hadrons, only normal thresholds and poles appear to be important.* The dual-resonance model is the living epitome of this. In fact, the dominance of normal singularities might serve as a precise definition of the bootstrap. Surely the bootstrap hypothesis would never have been formulated in a world dominated by anomalous singularities.

There might exist amplitudes in which both anomalous and normal singularities are important. In  $\pi\Sigma \rightarrow \pi\Sigma$ , for example, the  $t$  channel has a ( $K-N$ ) anomalous singularity, but the  $s$  channel is nonexotic and contains several resonances.

4. *Nuclear reactions have Regge behavior at very high energy.* In exotic-exchange reactions, a Regge cut is likely to dominate over the Regge trajectory associated with low-energy potential scattering.

5. *The asymptotically leading diagram also leads in the resonance region.* It would be very unsmooth for the leading diagram to suddenly lose its dominance. An extrapolation of the asymptotic behavior should average the bumps in the resonance region. However, due to the dominance of anomalous singularities, *nuclear reactions are not dual*, because the high-energy Regge behavior is *not* built up from *real* resonances.

6. *The amplitude factorizes in the  $t$  channel, at least for nonexotic exchange.*

7. *Below the threshold for pion production, we can revert back to old-fashioned nuclear physics.*

These rules provide a fairly well-defined framework for calculating high-energy nuclear cross sections. Our program is to push these hypotheses as far as possible, and to look for a possible breakdown. If they hold true, then  $B \leq 1$  hadrons would occupy an aristocratic status, while nuclei would be strictly composite. These are the stakes.

It may eventually prove necessary to distinguish two types of hadrons: those associated with a nearby threshold, and those, like  $p, \rho, \pi$ , etc., whose nature seems to be determined by global considerations. Rajasekaran<sup>80</sup> has suggested that global states correspond to poles in the  $K$  matrix,

whereas threshold-associated states do not. Of course, both types are poles in the  $S$  matrix.

The trouble with this classification is that there are several well-established nucleon resonances that fit nicely into the quark dual-resonance picture, yet appear to be intimately connected with a particular threshold. This ambiguity does not apply to exotic states, such as nuclei, hypernuclei, and  $Z^*$ 's, which should not even exist in the quark model.

The quark model may still have some relevance for the nuclear potential. The potential is known to transform as an  $SU(2)$  singlet, but what about  $SU(3)$ ? It is probably badly broken, but it might be broken in a simple way, such that the potential transforms, say, as the eighth component of an

octet.<sup>1</sup> This is quite possible, since the potential, which is due to meson exchanges, is very sensitive to the meson masses, and these are split by a medium-strong interaction transforming as the eighth component of an octet.

#### ACKNOWLEDGMENTS

This work was initiated at the Enrico Fermi Institute, the University of Chicago, and was completed at the Lawrence Berkeley Laboratory, the University of California during the summer of 1972. I thank G. F. Chew for Berkeley support and for a stimulating conversation, and K. A. Klare for computational assistance.

\*Work supported in part by the U. S. Atomic Energy Commission.

<sup>1</sup>G. W. Barry, *Ann. Phys. (N.Y.)* **73**, 482 (1972), referred to as I in the text.

<sup>2</sup>R. J. Glauber, in *High-Energy Physics and Nuclear Structure*, edited by S. Devons (Plenum, New York, 1970), p. 207, and references cited therein.

<sup>3</sup>E. S. Abers, H. Burkhardt, V. L. Teplitz, and C. Wilkin, *Nuovo Cimento* **42**, 365 (1966).

<sup>4</sup>L. Bertocchi and A. Capella, *Nuovo Cimento* **A51**, 369 (1967).

<sup>5</sup>In obtaining the last term,  $T_{\pi N}$  was assumed to be imaginary and insensitive to the integration variable.

<sup>6</sup>F. Gross, *Phys. Rev.* **134**, B405 (1964); **136**, B140 (1964); **140**, B410 (1965).

<sup>7</sup>N. W. Tanner, in *High-Energy Physics and Nuclear Structure*, edited by S. Devons (Ref. 2), p. 346.

<sup>8</sup>D. S. Koltun, in *Advances in Nuclear Physics*, edited by M. Baranger and E. Vogt (Plenum, New York, 1969), Vol. 3, p. 71.

<sup>9</sup>F. Becker and Yu. A. Batusov, *Riv. Nuovo Cimento* **1**, 309 (1971).

<sup>10</sup>A. Reitan, CERN Report No. CERN-TH-1409 (unpublished).

<sup>11</sup>T. Yao, *Phys. Rev.* **134**, B454 (1964).

<sup>12</sup>E. Ferrari and F. Selleri, *Nuovo Cimento* **27**, 1450 (1963).

<sup>13</sup>V. M. Kolybasov and N. Ya. Smorodinskaya, *Phys. Letters* **37B**, 272 (1971).

<sup>14</sup>H. L. Anderson, M. S. Dixit, H. J. Evans, K. A. Klare, D. A. Larson, M. V. Sherbrook, R. L. Martin, D. Kessler, D. E. Nagle, H. A. Thiessen, C. K. Hargrove, E. P. Hincks, and S. Fukui, *Phys. Rev. D* **3**, 1536 (1971).

<sup>15</sup>J. Chahoud, G. Russo, and F. Selleri, *Phys. Rev. Letters* **11**, 506 (1963).

<sup>16</sup>H. L. Anderson, M. Dixit, H. J. Evans, K. A. Klare, D. A. Larson, M. V. Sherbrook, R. L. Martin, D. Kessler, D. E. Nagle, H. A. Thiessen, C. K. Hargrove, E. P. Hincks, and S. Fukui, *Phys. Rev. Letters* **26**, 108 (1971).

<sup>17</sup>J. V. Allaby, F. Binon, A. N. Diddens, P. Duteil,

A. Klovning, R. Mennier, J. P. Peigneux, E. J. Sacharidis, K. Schlüpmann, M. Spighele, J. P. Stroot, A. M. Thorndike, and A. M. Wetherell, *Phys. Letters* **29B**, 198 (1969).

<sup>18</sup>U. Amaldi, R. Biancastelli, C. Bosio, G. Matthiae, J. V. Allaby, A. N. Diddens, R. W. Dobinson, A. Klovning, J. Litt, L. S. Rochester, K. Schlüpmann, and A. M. Wetherell, *Lett. Nuovo Cimento* **4**, 121 (1972).

<sup>19</sup>S. Mandelstam, *Proc. Roy. Soc. (London)* **A244**, 491 (1958).

<sup>20</sup>R. A. Arndt, *Phys. Rev.* **165**, 1834 (1968).

<sup>21</sup>G. F. Chew (unpublished).

<sup>22</sup>C. Richard-Serre, W. Hirt, D. F. Measday, E. G. Michaelis, M. J. M. Saltmarsh, and P. Skarek, *Nucl. Phys.* **B20**, 413 (1971).

<sup>23</sup>N. S. Craigie and C. Wilkin, *Nucl. Phys.* **B14**, 477 (1969).

<sup>24</sup>E. Coleman, R. M. Heinz, O. E. Overseth, and D. E. Pellet, *Phys. Rev.* **164**, 1655 (1967).

<sup>25</sup>G. Alberi, L. Bertocchi, and M. A. Gregorio, *Nuovo Cimento* **A10**, 37 (1972).

<sup>26</sup>K. Vasavada, *Ann. Phys. (N.Y.)* **34**, 191 (1965).

<sup>27</sup>J. Chahoud, G. Russo, and F. Selleri, *Nuovo Cimento* **45**, 38 (1966).

<sup>28</sup>D. Schiff and J. Tran Thanh Van, *Nucl. Phys.* **B5**, 529 (1968).

<sup>29</sup>H. Lee, *Phys. Rev.* **174**, 2130 (1968).

<sup>30</sup>N. E. Booth, C. Dolnick, R. J. Esterling, J. Parry, J. Scheid, and D. Sherden, *Phys. Rev. D* **4**, 1261 (1971).

<sup>31</sup>C. Dolnick, *Nucl. Phys.* **B22**, 461 (1970).

<sup>32</sup>Suggested to me by V. L. Telegdi.

<sup>33</sup>Data taken from J. C. Keck and A. V. Tollestrup, *Phys. Rev.* **101**, 360 (1956).

<sup>34</sup>D. J. George, *Phys. Rev.* **167**, 1357 (1968).

<sup>35</sup>M. E. Schillaci and R. Silbar, *Phys. Rev.* **171**, 1764 (1968).

<sup>36</sup>N. R. Nath, H. J. Weber, and P. K. Kabir, *Phys. Rev. Letters* **26**, 1404 (1971); N. R. Nath *et al.*, *Lett. Nuovo Cimento* **4**, 131 (1972).

<sup>37</sup>C. Schmid, *Phys. Rev.* **154**, 1363 (1967).

<sup>38</sup>M. Ruderman, *Phys. Rev.* **87**, 383 (1952).



- <sup>39</sup>S. A. Bludman, Phys. Rev. 94, 1722 (1954).
- <sup>40</sup>C. H. Q. Ingram, N. W. Tanner, J. J. Domingo, and J. Rohlin, Nucl. Phys. B31, 331 (1971).
- <sup>41</sup>J. Rohlin, K. Gabathuler, N. W. Tanner, C. R. Cox, and J. J. Domingo (unpublished).
- <sup>42</sup>W. J. Frank, K. C. Bandtel, R. Madey, and B. J. Moyer, Phys. Rev. 94, 1716 (1954).
- <sup>43</sup>K. R. Chapman, J. D. Jafar, G. Martelli, T. J. Macmahon, H. B. van der Raay, D. H. Reading, R. Rubenstein, K. Ruddick, D. G. Ryan, W. Galbraith, and P. Sharp, Nucl. Phys. 57, 499 (1964).
- <sup>44</sup>A. V. Crewe, B. Ledley, E. Lillethun, S. M. Marowitz, and C. Rey, Phys. Rev. 118, 1091 (1960).
- <sup>45</sup>D. Harting, J. C. Kluyver, A. Kusumegi, R. Rigopoulos, A. M. Sachs, G. Tibell, G. Vanderhaeghe, and G. Weber, Phys. Rev. 119, 1716 (1960).
- <sup>46</sup>Y. K. Akimov, O. V. Savchenko, and L. M. Soroko, Zh. Eksp. Teor. Fiz. 38, 643 (1960) [Sov. Phys. JETP 11, 462 (1960)].
- <sup>47</sup>N. Booth, Phys. Rev. 132, 2305 (1963).
- <sup>48</sup>M. Verde, Helv. Phys. Acta. 22, 339 (1949).
- <sup>49</sup>L. I. Schiff, Phys. Rev. 133, B802 (1964).
- <sup>50</sup>P. Picozza, C. Schaerf, R. Scrimaglio, G. Goggi, A. Piazzoli, and D. Scannicchio, Nucl. Phys. A157, 190 (1970).
- <sup>51</sup>K. Gabathuler, J. Rohlin, J. J. Domingo, C. H. Q. Ingram, S. Rohlin, and N. W. Tanner, Nucl. Phys. B40, 32 (1972).
- <sup>52</sup>J. J. Domingo, B. W. Allardyce, C. H. Q. Ingram, S. Rohlin, N. W. Tanner, J. Rohlin, E. M. Rimmer, G. Jones, and J. P. Girardeau-Montaut, Phys. Letters 32B, 309 (1970).
- <sup>53</sup>V. Chabaud, A. Eide, P. Lehrmann, A. Lundby, S. Mukhin, J. Myrheim, C. Baglin, P. Briandet, P. Fleury, P. Carlson, E. Johansson, M. Davier, V. Gracco, R. Morand, and D. Treille, Phys. Letters 38B, 449 (1972).
- <sup>54</sup>A. M. Sachs, H. Winick, and B. A. Wooten, Phys. Rev. 109, 1733 (1958).
- <sup>55</sup>K. C. Rogers and L. M. Lederman, Phys. Rev. 105, 247 (1957).
- <sup>56</sup>E. G. Pewitt *et al.*, Phys. Rev. 131, 1826 (1963).
- <sup>57</sup>J. H. Norem, Nucl. Phys. B33, 512 (1971).
- <sup>58</sup>L. S. Dul'kova, I. B. Sokolova, and M. G. Shafranova, Zh. Eksp. Teor. Fiz. 35, 313 (1959) [Sov. Phys. JETP 8, 217 (1959)].
- <sup>59</sup>L. S. Schroeder, D. G. Crabb, R. Keller, J. R. O'Fallon, T. J. Richards, R. J. Ott, J. Trischuk, and J. Va'vra, Phys. Rev. Letters 27, 1813 (1971).
- <sup>60</sup>C. Carlson, Phys. Rev. C 2, 1224 (1970).
- <sup>61</sup>W. R. Gibbs, Phys. Rev. C 3, 1127 (1971).
- <sup>62</sup>G. Alberi and L. Bertocchi, Nuovo Cimento A 63, 285 (1969).
- <sup>63</sup>M. Davier, D. Benaksas, D. Drickey, and P. Lehmann, Phys. Rev. 137, B119 (1965).
- <sup>64</sup>There are very preliminary data from Saclay up to 1.2 GeV.
- <sup>65</sup>V. I. Komarov, G. E. Kosarev, and O. V. Savchenko, Yad. Fiz. 11, 711 (1970) [Sov. J. Nucl. Phys. 11, 399 (1970)].
- <sup>66</sup>B. Z. Kopeliovich and I. K. Potashnikova, Yad. Fiz. 13, 1032 (1971) [Sov. J. Nucl. Phys. 13, 592 (1971)].
- <sup>67</sup>V. I. Komarov, G. E. Kosarev, and O. V. Savchenko, Yad. Fiz. 12, 1229 (1970) [Sov. J. Nucl. Phys. 12, 675 (1971)].
- <sup>68</sup>D. E. Dorfan, J. Eades, L. M. Lederman, W. Lee, C. C. Ting, P. Piroué, S. Smith, J. L. Brown, J. A. Kadyk, and G. H. Trilling, Phys. Rev. Letters 14, 995 (1965).
- <sup>69</sup>D. I. Blokhintsev, Zh. Eksp. Teor. Fiz. 33, 1295 (1957) [Sov. Phys. JETP 6, 995 (1958)]; D. I. Blokhintsev and K. A. Toktarov, JINR Report No. R4-4018, 1968 (unpublished).
- <sup>70</sup>K. W. Ford and J. A. Wheeler, Ann. Phys. (N.Y.) 7, 259 (1959); R. G. Newton, *Scattering Theory of Waves and Particles* (McGraw-Hill, New York, 1966).
- <sup>71</sup>H. C. Bryant and N. Jarmie, Ann. Phys. (N.Y.) 47, 127 (1968).
- <sup>72</sup>J. F. Reading and W. H. Bassichis, Phys. Rev. D 5, 2031 (1972).
- <sup>73</sup>H. H. Heckman, D. E. Greiner, P. J. Lindstrom, and F. S. Bieser, Phys. Rev. Letters 28, 926 (1972).
- <sup>74</sup>Yu. M. Goryachev, V. P. Kanavets, I. I. Levintov, B. V. Morozov, N. A. Nikiforov, and A. S. Starostin, Yad. Fiz. 11, 629 (1970) [Sov. J. Nucl. Phys. 11, 353 (1970)].
- <sup>75</sup>Yu. M. Antipov, S. P. Denisov, S. V. Donskov, Yu. P. Gorin, V. A. Kachanov, V. P. Khromov, V. M. Kutijin, L. G. Landsberg, V. G. Lapshin, A. A. Morozov, A. I. Petrukhin, Yu. D. Prokoshkin, E. A. Razuvaev, V. I. Rykalin, V. I. Solyanik, D. A. Stoyanova, R. S. Shuvalov, N. K. Vishnevsky, F. A. Yetch, and A. M. Zaytzev, Phys. Letters 34B, 164 (1971).
- <sup>76</sup>D. E. Dorfan, J. Eades, L. M. Lederman, W. Lee, and C. C. Ting, Phys. Rev. Letters 14, 1003 (1965).
- <sup>77</sup>Yu. M. Antipov, N. Vishnevskii, Yu. P. Gorin, S. P. Denisov, S. V. Donskov, F. A. Ech, G. D. Zhilchenkova, A. M. Zaitsev, V. A. Kachanov, V. M. Kut'in, L. G. Landsberg, V. G. Lapshin, A. A. Lebedev, A. G. Morozov, A. I. Petrukin, Yu. D. Prokoshin, E. A. Razuvaev, V. I. Rykalin, V. I. Solyanik, D. A. Stoyanova, V. P. Khromov, and R. S. Shuvalov, Yad. Fiz. 12, 311 (1970) [Sov. J. Nucl. Phys. 12, 171 (1971)].
- <sup>78</sup>A. K. Kerman and L. S. Kisslinger, Phys. Rev. 180, 1483 (1969).
- <sup>79</sup>L. A. Kondratyuk and I. S. Shapiro, Yad. Fiz. 12, 401 (1970) [Sov. J. Nucl. Phys. 12, 220 (1971)].
- <sup>80</sup>G. Rajasekaran, Phys. Rev. D 5, 610 (1972).